Published in final edited form as:
Atherosclerosis. 2010 July ; 211(1): 122–129. doi:10.1016/j.atherosclerosis.2010.04.005.

Lyso-phosphatidylcholine induces osteogenic gene expression and phenotype in vascular smooth muscle cells

Kasey C. Vickers[1], **Fernando Castro-Chavez**[1], and **Joel D. Morrisett**[1,2]

[1]Department of Medicine, Biology Baylor College of Medicine, Houston, TX

[2]Department of Medicine Biochemistry/Molecular Biology Baylor College of Medicine, Houston, TX

Abstract

Objective: Calcifying vascular cells in human atherosclerotic plaques actively contribute to ectopic vascular mineralization. Lyso-phosphatidylcholine (LPC), a product of oxidized phosphatidylcholine hydrolysis, is found at concentrations of 1-12μg/g tissue throughout the atheroma. The objective of this study was to determine if LPC induces an osteogenic phenotype in vascular smooth muscle cells.

Methods and Results: Proliferating human aortic smooth muscle cells were treated with a wide-range of LPC concentrations (0.1nM-100μM) over 14 days. Von Kossa, Alizarin Red S, and alkaline phosphatase staining were used to identify mineralizations. RT-PCR, ELISA, alkaline phosphatase activity, and ^{45}Ca incorporation assays were used to evaluate the osteo-inductive effect of LPC on smooth muscle phenotype. Histology and morphometry revealed that cells treated with as little as 10nM LPC produced calcium phosphate deposits in culture. LPC-treated vascular smooth muscle cells showed a significant increase in ^{45}Ca incorporation and alkaline phosphatase activity. Furthermore, LPC treatment induced a significant loss of Schnurri 3 protein, a key repressor of Runt-related transcription factor 2 stability. Genomic studies revealed that osteogenic gene expression was significantly up-regulated in LPC-treated cells, which is attributed to increased Runt-related transcription factor 2 expression and transcriptional activity.

Conclusion: LPC induces osteogenic morphology, physiology, gene expression, and phenotype in vascular smooth muscle cells. The present study suggests that localized concentrations of LPC in human atherosclerotic plaques may be a contributing factor to the generation of calcifying vascular cells.

Keywords

lyso-phosphatidylcholine; vascular calcification; calcifying vascular cells; atherosclerosis; smooth muscle cells

Correspondence to: Joel D. Morrisett 6550 Fannin St. FB A679D MS-A601 Methodist Hospital Houston, TX 77030 T(713)-798-4164 F(713)-798-4121 morriset@bcm.tmc.edu.

Vickers: LPC induces VSMC osteogenesis.

1. Introduction

Vascular calcification is an ectopic process of soft tissue osteogenesis, most notably associated with atherosclerosis and the driving force of inflammation [1]. Atherosclerosis-associated vascular calcification is a clinical indicator of advanced atherosclerosis, and its presence increases the pathological burden of the disease and increases negative clinical outcomes [2-4]. Evidence suggests that the formation of calcification, usually in the form of calcium hydroxyapatite, can occur through both passive and active mechanisms in the arterial wall [5]. Nevertheless, it is likely that most atherosclerosis-associated calcification results from active cellular processes that are both highly regulated and organized. Calcifying vascular cells (CVCs) in the atherosclerotic plaque synthesize and secrete many osteogenic proteins into the extracellular matrix. Cellular contributions range from structural proteins that prepare the environment for mineralization nucleation, to enzymes and regulatory proteins. The origin and lineage of CVCs has been extensively debated [6-8]. Although it is possible that circulating osteoblast precursors or resident mesenchymal stem cells have the potential to produce ectopic calcification, it is more likely that CVCs arise from a subpopulation of vascular smooth muscle cells (VSMCs) in response to environmental stimuli.

The atherosclerotic lesion environment is characterized by severe inflammation and the accumulation of lipids. The greatest source of lipid to the atheroma is likely modified LDL. Modified LDL and products resulting from its breakdown have been shown to exert many effects upon VSMC physiology and phenotype [9]. One specific lipid, lyso-phosphatidylcholine (LPC), is a strong candidate for stimulating VSMCs to transition into an osteogenic (CVC) phenotype. In the atheroma, one source of LPC is the enzymatic hydrolysis of phosphatidylcholine by secreted phospholipases, including phospholipase A_2 (s) (sPLA$_2$-IIA or sPLA$_2$-V) and lipoprotein-associated phospholipase A_2 (Lp-PLA$_2$) [10-12]. Oxidation of LDL phosphatidylcholine results in a shortened *sn*-2 acyl chain, which serves as the distinctive substrate for Lp-PLA$_2$ lipolysis to produce LPC and oxidized fatty acids [13]. It is widely held that LPC is the bioactive component responsible for various responses by atheroma cells to residential oxidized LDL [14]. Previous studies have shown that atherosclerotic lesions have a substantial concentration of LPC, which is proportional to the extent of the disease [15,16]. Furthermore, symptomatic carotid atherosclerotic plaques have been reported to contain 2-fold higher levels of LPC than plaques of asymptomatic patients [17]. The smooth muscle cell (SMC) response to LPC in culture is dynamic, and affects many cellular processes. Cell migration [18], intracellular calcium flux $[Ca^{2+}]_I$ [19], and inflammatory activation states [20] have all been shown to be altered by LPC stimulation in cultured SMCs. Furthermore, LPC has been demonstrated to activate the p38 [21] and ERK [22] MAP Kinase pathways in VSMCs. Significantly, the p38 MAPK pathway has been shown to be essential for osteoblast differentiation [23]. Therefore, LPC is a strong candidate for inducing osteogenic transitions in VSMCs and undoubtedly plays a significant role in the pathophysiology of atherosclerosis; however, its role in vascular calcification has not been characterized. In this study, we demonstrate that LPC induces the transition of VSMCs into an osteogenic phenotype, which ultimately leads to the nucleation and deposition of extracellular calcium phosphate.

2. Materials and methods

2.1. Cell culture

Human aortic smooth muscle cells (proliferating, p4) were purchased from Clonetics (Lonza). Cells were maintained in SmGM-2 media with supplements: hEGF, Insulin, hFGF-B, TGF-B1, Heparin, 15% FBS, GA-1000 (Lonza). Cells were cultured, 24-well or 6-well plates, in the following media for the duration of the experiments: DMEM (4.5g/L D-glucose, L-glutamine, 110mg/L sodium pyruvate) supplemented with 15% FBS, 100U/mL penicillin/streptomycin, 25ng/mL amphotericin B, and 0.1μM insulin. In addition, selected plates

received calcifying media supplements 10mmol/L β-glycerophosphate (Sigma) and 50ng/mL ascorbic acid. The LPC-treated cultures received L-α-lysophosphatidylcholine (L-α-lysolecithin, Type I, 99%, Sigma) concentrations from 0.1nM-100μM. The media was changed every other day for 14 days. LPC purity was assessed by thin-layer chromatography and gas chromatography / mass spectrometry (GC-MS) (Supplemental methods 1).

2.2. Quantification of LPC in human CEA tissue segments

Carotid endarterectomy (CEA) tissues were excised from patients undergoing unilateral endarterectomy at The Methodist Hospital, Houston, TX. This work was approved by the Baylor College of Medicine institutional review board for human research. The atheromatous CEA tissues were stored in RNALater at 4°C overnight then RNALater was removed and wet tissues were stored at −80°C. When needed, the tissues were cut anatomically into common, bifurcation, internal, and external segments. Weighed CEA segments (200-500mg) were homogenized in 3mL $CHCl_3$:CH_3OH (2:1) containing 1% butylated hydroxytoluene using a Brinkman Polytron. After 30sec homogenization, solids were allowed to settle after which the supernatant was decanted and the pellet stored at 4°C. The extraction procedure was repeated 2X and all three extracts were combined and evaporated to dryness. The dry extract was redissolved in 1ml $CHCl_3$:CH_3OH (10:1) and 5μl was applied to a thin-layer chromatography plate (20×20cm) which was first eluted with $CHCl_3$:CH_3OH:H_2O (65:24:4), then with hexane:diethyl ether:acetic acid (75:35:1). To visualized lipids, the plate was sprayed with primuline (5% in acetone:water (80:20) and scanned with a Storm Phosphoimager 840 (Molecular Dynamics). LPC was quantified from a standard curve.

2.3. Calcification quantification, staining and morphometry

Pellets remaining from the lipid extraction (see above) were washed 2X and finally suspended in 2ml distilled water. Calcium in the washes and suspensions were quantified with the Calcium Arsenazo III kit (Pointe Scientific, Inc)

Chemical staining for calcium was performed in 6-well culture plates. Von Kossa (Supplemental methods 2.A) and Alizarin Red S (ARS, Supplemental methods 2.B) reagents were each used to stain in-well calcium phosphate deposits. Cells were imaged using a Leica DC300 digital camera attached to a Leitz microscope (4X). Morphometric techniques were used to ARS stained wells to quantify LPC-induced VSMC mineralization. Transparent numbered grids (1×1mm) were placed beneath clear 6-well plates. Random boxes were selected (n=10, random number generator) and scored positive by the presence of an ARS positive calcific ridge or nodule touching at least one edge of the box.

In VSMC cultures (35mm wells), LPC-treated and untreated cells were washed (3X TBS) then scraped with 1mM Octyl Glucoside (n-octyl Beta-D-glucopyranoside). Harvested cells were analyzed for total calcium (Arsenazo-III kit) and total phosphate (Anaspec Sensolyte MG phosphate kit) (Supplemental methods 3). Total protein was determined using the BCA reagent kit (Pierce). Cellular calcium and phosphate were normalized to protein concentration

2.4. RNA and protein isolation

Total RNA was isolated from cell culture wells using Trizol and Qiagen RNAeasy columns. RNA concentrations were determined by NanoDrop® spectroscopy. Cells for protein analysis were rinsed with 1X PBS and lysed with protein extraction buffer (pH 7.4) for 5 min (Supplemental methods 4). Total protein was quantified using the Bio-Rad D_C Protein Assay. Osteopontin concentrations were determined using the IBL Human Osteopontin EIA Kit (Immuno-Biological Laboratories Co., Japan).

Schnurri 3 was quantified using a novel Schnurri 3 ELISA, developed in-house utilizing two Schnurri 3 antibodies, SHNA and SHNB (Supplemental methods 5). Concentrations of human osteopontin and Schnurri 3 were normalized to total protein concentrations (μg/μg total protein).

2.5. Real-time PCR

Total RNA (<1μg) was reverse-transcribed with random primers using Superscript III (Invitrogen). Protocol for first strand cDNA synthesis only was performed followed by RNaseH treatment for 20min at 37°C. Resulting cDNA was diluted (1:5) and used as template (2μL) in 25μL real-time PCR reactions with SYBR Green PCR Master Mix (Applied Biosystems). Optimized primers (10μM, 1μL) were used in the real-time PCR reactions (sequences, Supplemental methods 6) on an ABI Prism 7000 sequence detection system (Applied Biosystems). Relative quantitative analysis (2^{-ddCt}) was performed by normalizing data to the housekeeping gene PP1A (dCt). Initial (pre-induced) gene expression levels (dCt) for each gene of interest were used as calibrators (ddCt). Fold changes for experimental treatments were determined relative to untreated VSMCs.

2.6. Alkaline phosphatase activity

Alkaline phosphatase activity (in well) was determined using the Alkaline Phosphatase Substrate Kit (Bio-Rad) with 2mL (well) volumes (6-well plate). Color development was achieved by 37°C incubation for 30min. Cells were rinsed 3X with ddH_2O and imaged as described above. Alkaline phosphatase was extracted from cell culture wells using 1mM Octyl Glucoside (n-octyl Beta-D-glucopyranoside). Alkaline phosphatase activity was quantified using SensoLyte™ (AnaSpec) FDP Detection fluorometric assay kit and mass was quantified using the Alkaline Phosphatase Substrate Kit (Bio-Rad) (as per instructions).

2.7. Calcium incorporation assay

$^{45}CaCl_2$ was purchased through American Radiolabeled Chemicals, Inc. (St. Louis, MO). The radiolabeled calcium (1μCi/mL $^{45}CaCl_2$) was added to the media 48hrs prior to sampling. Media was aspirated and cells were rinsed twice with 1X PBS. Cells were scraped/collected, lysed with 0.2N NaOH, 1% SDS (37°C, 45min) and neutralized with 0.2N HCl. Radioactivity was measured in 100μl samples with 2mL scintillation fluid (ScintiVerse, Fisher). Samples were counted using a liquid scintillation counter (Beckman LS6000IC, 5 min counts). CPM was normalized to total protein concentration (CPM/μg total protein).

2.8. RUNX2-Luciferase reporter assay

Osteogenic reporter assays were used to test the induction of RUNX2 transcriptional activity during LPC stimulation of VSMCs. The reporter construct, p6OSE2-luc (6x OSE2 of osteocalcin promoter) and control vehicle pluc4, were gifts from Gerard Karsenty (Columbia Univ.) and have been previously described [24]. Transient transfection protocols are described in Supplemental Methods 7.

2.9. Statistical analysis

All values are expressed as mean ±SD. A value $p < 0.05$ was considered statistically significant. When comparing only two groups a Mann-Whitney (non-parametric) t-test, two-tailed with 95% confidence was used. We used one-way ANOVA (non-parametric test) with a Newman-Keuls post-test (95% confidence) when comparing groups >2, with exception of gene expression studies (RQV). Normality of data was determined by normal probability plots.

3. Experimental Results

3.1. LPC is abundant in CEA tissue segments and correlates to calcification

LPC was quantified in CEA segments using thin-layer chromatography (arrow, Fig.1A). A standard curve (LPC) was used to determine the distribution of 1-12μg LPC/g tissue in each CEA segment. The internal and bifurcation segments, segments that often possess the most extensive calcification, had the highest LPC concentration per wet weight of tissue. Total calcification was measured in CEA segments as the sum of calcium in the soluble supernatant and the insoluble pellet. A significant correlation (R=0.723, p=0.023, n=14) was observed between LPC (μg) and total calcium (μg) in CEA tissue segments (Fig.1B).

3.2. LPC induces VSMCs to form calcific nodules in culture

Prior to LPC treatment, VSMCs were characterized in order to validate the starting phenotype by using antibodies to specific cell markers. VSMCs were positive for SM α-Actin (Supplemental data 1) and SM myosin heavy-chain; and negative for CD68, CD31, and VE Cadherin as determined by immunohistochemistry (data not shown). The effect of LPC on VSMCs was investigated by supplementing culture media with LPC spanning a 10^6-fold range of concentrations (0.1nM-100μM). After 14 days, cells treated with 1-10nM LPC showed the largest morphological differences (Supplemental data 1). At approximately day 10, confluent LPC-treated cells started to form large nodules and pronounced ridges. Untreated cells also developed comparable structures over the 14 day treatment; however these structures were much smaller, less organized, and less abundant than the LPC-treated cells (Fig.1C). VSMC-contributed mineralization was quantified in culture using morphometric techniques. A numbered grid (1×1mm) was placed under VSMC culture plates after ARS calcium phosphate staining. Random boxes were selected (random number generator) and positive mineralizations were counted by the presence of a ridge or cluster of mineralization crossing at least one edge of the selected boxes. Out of the possible 10 selected boxes for LPC-treated VSMCs (10nM), all 10 were considered positive (10/10) (Fig.1C). In contrast, only 4 out of 10 boxes were positive for the untreated VSMCs (Fig.1C). VSMCs have been characterized previously with respect to morphological changes induced by β-glycerophosphate treatments. In our experiments, VSMCs treated with LPC underwent morphological changes similar to those induced by β-glycerophosphate (Supplemental data 2) [25].

To determine if LPC-treated cells produce calcium phosphate deposits *in vitro*, we used von Kossa and ARS stains. Both LPC (10nM) (Fig.2A) and β-glycerophosphate (1mM)-treated cells (Supplemental data 2) were positive for von Kossa calcium phosphate staining. In contrast, untreated VSMCs showed very little or no positive staining for calcium phosphate using von Kossa (Fig.2A). LPC (10nM)-treated cells also stained positive for ARS stain, confirming the presence of calcium deposits (Fig.2B); which was most concentrated in organized ridges and nodules (arrows). Untreated VSMC cultures showed no extracellular calcium deposition in ARS stained wells (Fig.2B). Furthermore, total phosphate (Fig.2C) and calcium levels were markedly increased in LPC (10nM)-treated wells compared to controls (Supplemental data 3). There were no differences in calcium or phosphate concentrations in culture media conditions.

3.3. LPC induces VSMCs to transition towards an osteogenic phenotype

To test the capacity of LPC to induce matrix mineralization in culture, a feature of both osteoblasts and CVCs, we used a $^{45}CaCl_2$ calcium incorporation assay. LPC (1nM)-treated cells had significantly higher calcium incorporation (p<0.001) than both untreated and β-glycerophosphate-treated cells (Fig.2D). 1nM LPC showed the highest incorporation compared to the other LPC concentrations, but all LPC concentrations (0.1nM-100nM) were significantly higher than the untreated cells (p < 0.01).

3.4. LPC induces osteogenic gene expression in VSMCs

LPC-treated cells (10nM) were observed to have a significantly higher expression of alkaline phosphatase mRNA (15.3-fold) compared to untreated VSMCs ($p<0.05$, Fig.3A). Collagen 1α, a specific collagen involved in osteogenesis, was markedly increased in VSMCs treated with LPC (10nM p=0.06; 1nM $p<0.05$, 0.1nM $p<0.05$ Fig.3B). Osteopontin, a highly acidic glycoprotein secreted by osteoblasts, was also up-regulated (4.7-fold) in LPC-treated cells (10nM $p<0.05$, Fig.3C). Osteopontin ELISA assays confirmed that the up-regulation in osteopontin mRNA translated to a significant increase in osteopontin protein ($p<0.01$, Fig.3D).

3.5. VSMCs treated with LPC show a marked increased in alkaline phosphatase activity

LPC (10nM)-treated VSMCs were observed to have a higher level of alkaline phosphatase activity compared to untreated cells (Fig.4A). Alkaline phosphatase is a key osteogenic enzyme; through its actions it provides the limited free phosphate for the formation of hydroxyapatite. At 1X the digital images of LPC-treated cells looked very similar to β-glycerophosphate-treated cells; both showed significantly darker staining than untreated cells (Fig.4A). Under higher magnification (10X) the LPC-treated cells exhibited alkaline phosphatase activity on the large organized structures in the cell culture dish including ridges and nodules (Fig.4A). These observed changes in alkaline phosphatase activity are likely due to a substantial increase in alkaline phosphatase mass (Fig.4B) and specific activity (Fig.4C,D). These data are consistent with the significant increase in alkaline phosphatase gene expression (mRNA) observed in LPC (10nM)-treated cells (Fig.3A).

3.6. RUNX2 expression and transcriptional activity are increased in LPC-treated VSMCs

Runt-related transcription factor 2 (RUNX2), a mammalian homologue of *Drosophila* runt, is an osteoblast master transcription factor [26]. RUNX2 gene expression (mRNA) was increased in all LPC conditions, from 1nM to 100nM, compared to untreated cells (10nM $p<0.05$, Fig. 5A). It is of particular interest that RUNX2 expression is up-regulated by LPC treatment because RUNX2 doesn't control its own expression. Furthermore, osteo-inductive β-glycerophosphate failed to induce a significant increase in VSMC RUNX2 expression (Fig. 5A).

Increased RUNX2 transcriptional activity and the induction of osteogenic gene expression are characteristic features of VSMC osteogeneis [6,25]. As described above, many of RUNX2 transcriptional targets are up-regulated with LPC treatments (Fig.3AC). RUNX2 regulates and controls osteogenic gene expression through promoter OSE (osteoblast-specific element) response elements in osteoblasts and CVCs. To determine if LPC-induced osteogenic gene expression changes are mediated through the transcriptional actions of RUNX2, we used a p6OSE2-luciferase reporter assay. Cells treated with 0.1-10nM LPC exhibited a significant increase in RUNX2 transcriptional activity compared to untreated cells ($p<0.001$, Fig.5B), and peaked with 10nM LPC treatment. In addition, RUNX2 transcriptional activity was monitored over the course of the temporal experiment. LPC (10nM)-treated VSMCs at day 14 reported a significant increase in RUNX2 transcriptional activity compared to vehicle ($p<0.01$), 100nM LPC 14d ($p<0.05$), and untreated cells 14d ($p<0.05$) (Fig.5C). Increased RUNX2 activity over background in LPC (10nM)-treated cells was first observed at day 10; however, at day 14 LPC 0.1nM, 1nM, and 10nM all showed increased RUNX2 activity (Fig.5C).

Schnurri 3, an essential regulator of adult bone homeostasis, directly interacts with RUNX2 and negatively regulates the transcription factor's stability and expression [27]. To determine if LPC alters Schnurri 3 levels in VSMCs we used a novel Schnurri 3 ELISA. VSMCs treated with 10nM LPC reported a significant loss of Schnurri 3 protein (Fig.5D).

Collectively, these results demonstrate that LPC induces osteoblast-like changes in morphology, physiology, gene expression, and phenotype in VSMCs. Taken together, these data suggest that localized concentrations of LPC in the atherosclerotic lesion may induce VSMCs to transition into an osteogenic phenotype, thereby contributing to ectopic vascular calcification.

4. Discussion

Vascular smooth muscle cells are highly responsive to environmental stimuli that govern their cellular behavior. In this study, and in cell culture studies by others, VSMCs have clearly shown the capacity for osteogenic trans-differentiation. Cell culture studies demonstrate that the proposed osteo-inductive mechanisms are clearly possible in the developing plaque, whereby localized VSMCs respond to factors present in the atheroma by trans-differentiating or transitioning into osteogenic phenotypes.

The findings of this study suggest that specific biologically relevant concentrations of LPC may induce an osteogenic phenotype in VSMCs of the arterial wall. The results of the gene expression (Fig.3), calcium incorporation (Fig.4), and RUNX2 transcriptional activity (Fig.5) studies illustrate that the VSMC's response to LPC is not monotonic. These data suggest that the optimal LPC bioactive concentration for the greatest osteogenic transition response is 1-10nM. Other investigators have demonstrated that the optimal concentrations of other osteo-inducing agents are generally several orders of magnitude greater. For example the CVC-inducing concentration of β-glycerophosphate was reported as 10mM, one-hundred thousand-fold greater than LPC (10nM) [6,25]. In terms of induced gene expression and increased matrix mineralization, LPC had much greater efficacy than β-glycerophosphate. In our studies, these two agents were not synergistic or additive in cellular response.

LPC was observed to be abundantly present in the carotid atheroma (1-12μg/g) and significantly associated with vascular calcification (Fig.1); however, the complete mechanism of LPC-induced VSMC osteogenesis is currently unknown. One plausible mechanism could be explained by the relief of negative repression upon RUNX2, the master osteogenic transcription factor. Schnurri 3, also known as KRC, ZAS3, and HIVEP3, is a WWP1 E3 ubiquitin ligase recruiter for protein ubiquitination [27]. Schnurri 3 has been demonstrated to directly bind to RUNX2 and promote RUNX2 degradation through ubiquitination and subsequent destabilization [27]. Osteogenic VSMCs, treated with LPC (10nM), were observed to have a significant reduction of Schnurri 3 protein. The LPC-induced loss of Schnurri 3 protein likely confers part of the observed increase in RUNX2 transcriptional activity and subsequent increase in osteogenic gene expression.

Studies have demonstrated that LPC induces many physiological changes to VSMCs. Specifically, LPC has been shown to alter smooth muscle cellular physiology by raising intracellular calcium concentrations $[Ca^{2+}]i$, either by inducing calcium store release or extracellular calcium influx [19]. Chen *et. al* demonstrated that LPC induces an increase in intracellular calcium $[Ca^{2+}]_i$ in a dose-dependent manner (100nM - 10μM) at concentrations similar to our observations (Fig.2D); likely through extracellular calcium influx as opposed to intracellular calcium store release [19]. The lack of a rise in intracellular calcium concentrations $[Ca^{2+}]_i$ after LPC inductions in a calcium-free solution and the insensitivity of the LPC-induced increase in intracellular calcium $[Ca^{2+}]_i$ in the presence of a calcium store release inhibitor (TMB-8) support LPC induced calcium influx [19]. Consistent with these data, LPC (10nM)-treated VSMCs showed a significant increase in total calcium, when normalized to total protein (Supplemental data 3). Similar to LPC, 1,25-Dihydroxyvitamin D_3 also increases calcium influx and $[Ca^{2+}]i$ [28]. Correspondingly, 1,25-Dihydroxyvitamin D_3 has also been shown to drive VSMCs to an osteoblast-like phenotype [29]. Another potential mechanism for LPC-

induced osteogenic transition is through transmembrane signaling. At higher concentrations (>1μM) LPC is cytotoxic to VSMCs (data not shown). At lower concentrations (<1μM) LPC may interact with the plasma membrane and potentially signal through MAP kinase or Akt cascades [21,22]. These specific pathways have been shown to be essential for osteoblast differentiation [23]. Substantially more research is needed to resolve the potentially numerous mechanisms of LPC induction. Specifically, to determine exactly how LPC interacts with the VSMC, and how this signal is transmitted to the nucleus.

Once oxLDL becomes resident in the subintima due to its modified state, localized secretory phospholipases bound to VSMC proteoglycans ($sPLA_2$-V) and/or $LpPLA_2$ (free or LDL bound), enzymatically release pro-atherogenic LPC [12,13]. LPC is a direct product of the lipolysis of oxidized PC, the major phospholipid in LDL. Minimally modified LDL (mm-LDL) and acetylated LDL (Ac-LDL) have been demonstrated to induce osteogenic differentiation of VSMCs as well [30]. Hence, LPC may be the critical component originating from modified lipoproteins that subsequently induces osteogenic differentiation. Atherosclerotic plaques also possess the capacity to create small microenvironments where specific bioactive concentrations of molecules may develop. Furthermore, certain atherosclerotic plaques have many conduits for small molecule distribution. These concepts provide a mechanism of generation for LPC and a reasonable explanation for how osteo-inductive concentrations of this bioactive lipid may interact with VSMCs in the atherosclerotic plaque.

Here we present evidence that LPC induces up-regulation of osteogenic genes and proteins. This osteogenic up-regulation is likely mediated through increased activity of the master osteogenic transcription factor RUNX2, whose own expression is up-regulated in these models. Furthermore, increased RUNX2 transcriptional activity may also be attributed to LPC-induced loss of Schnurri 3, a negative regulator of RUNX2. LPC-induced VSMCs have increased alkaline phosphatase activity and increased calcium incorporation; both are hallmarks for matrix mineralization in culture. Furthermore, LPC-treated cells produce calcification in the form of calcium phosphate deposits in culture.

In summary, LPC induces VSMCs to appear and behave much like calcifying vascular cells in culture. The implication of this study is that LPC likely induces atherosclerosis-associated VSMCs to transition into an osteogenic phenotype in the atheroma, contributing to the formation and growth of ectopic vascular calcification. These observations confer a novel mechanism of osteogenesis in the vascular wall, and promote potential new treatment strategies that may be utilized for plaque stabilization and regression.

Supplementary Material

Refer to Web version on PubMed Central for supplementary material.

Acknowledgments

The authors acknowledge the assistance of Jennifer Jiang with alkaline phosphatase activity assays, Massa Chen with LPC measurements, and Eliseu Yung Chuang with cell culture experiments. This work was supported in part by National Institutes of Health, HL07812 and HL63090 (TTGA).

References

1. Doherty TM, Asotra K, Fitzpatrick LA, et al. Calcification in atherosclerosis: bone biology and chronic inflammation at the arterial crossroads. Proc Natl Acad Sci USA 2003;100:11201–11206. [PubMed: 14500910]
2. Abedin M, Tintut Y, Demer LL. Vascular calcification: mechanisms and clinical ramifications. Arterioscler Thromb Vasc Biol 2004;24:1161–1170. [PubMed: 15155384]

3. Prabhakaran S, Singh R, Zhou X, et al. Presence of calcified carotid plaque predicts vascular events: the Northern Manhattan Study. Atherosclerosis 2007;195:197–201.
4. Sangiorgi G, Rumberger JA, Severson A, et al. Arterial calcification and not lumen stenosis is highly correlated with atherosclerotic plaque burden in humans: a histologic study of 723 coronary artery segments using nondecalcifying methodology. J Am Coll Cardiol 1998;31:126–133. [PubMed: 9426030]
5. Speer MY, Giachelli CM. Regulation of cardiovascular calcification. Cardiovasc Pathol 2004;13:63–70. [PubMed: 15033154]
6. Steitz SA, Speer MY, Curinga G, et al. Smooth muscle cell phenotypic transition associated with calcification: upregulation of Cbfa1 and downregulation of smooth muscle lineage markers. Circ Res 2001;89:1147–1154. [PubMed: 11739279]
7. Abedin M, Tintut Y, Demer LL. Mesenchymal stem cells and the arterial wall. Circ Res 2004;95:671–676. [PubMed: 15459088]
8. Eghbali-Fatourechi GZ, Lamsam J, Fraser D, et al. Circulating osteoblast-lineage cells in humans. N Engl J Med 2005;352:1959–1966. [PubMed: 15888696]
9. Chatterjee S, Bhunia AK, Snowden A, Han H. Oxidized low density lipoproteins stimulate galactosyltransferase activity, ras activation, p44 mitogen activated protein kinase and c-fos expression in aortic smooth muscle cells. Glycobiology 1997;7:703–710. [PubMed: 9254052]
10. Zalewski A, Macphee C. Role of lipoprotein-associated phospholipase A2 in atherosclerosis: biology, epidemiology, and possible therapeutic target. Arterioscler Thromb Vasc Biol 2005;25:923–931. [PubMed: 15731492]
11. Rosenson RS, Gelb MH. Secretory phospholipase A2: a multifaceted family of proatherogenic enzymes. Curr Cardiol Rep 2009;11:445–451. [PubMed: 19863869]
12. Rosengren B, Jönsson-Rylander AC, Peilot H, et al. Distinctiveness of secretory phospholipase A2 group IIA and V suggesting unique roles in atherosclerosis. Biochim Biophys Acta 2006;1761:1301–1308. [PubMed: 17070102]
13. Tokumura A, Sumida T, Toujima M, et al. Structural identification of phosphatidylcholines having an oxidatively shortened linoleate residue generated through its oxygenation with soybean or rabbit reticulocyte lipoxygenase. J Lipid Res 2000;41:953–962. [PubMed: 10828088]
14. Kougias P, Chai H, Lin PH, et al. Lysophosphatidylcholine and secretory phospholipase A2 in vascular disease: mediators of endothelial dysfunction and atherosclerosis. Med Sci Monit 2006;12:RA5–16. [PubMed: 16369478]
15. Portman OW, Alexander M. Lysophosphatidylcholine concentrations and metabolism in aortic intima plus inner media: effect of nutritionally induced atherosclerosis. J Lipid Res 1969;10:158–165. [PubMed: 4238547]
16. Schmitz G, Ruebsaamen K. Metabolism and atherogenic disease association of lysophosphatidylcholine. Atherosclerosis 2010;208:10–18. [PubMed: 19570538]
17. Mannheim D, Herrmann J, Versari D, et al. Enhanced expression of Lp-PLA2 and lysophosphatidylcholine in symptomatic carotid atherosclerotic plaques. Stroke 2008;39:1448–1455. [PubMed: 18356547]
18. Kohno M, Yokokawa K, Yasunari K, et al. Induction by lysophosphatidylcholine, a major phospholipid component of atherogenic lipoproteins, of human coronary artery smooth muscle cell migration. Circulation 1998;98:353–359. [PubMed: 9711941]
19. Chen Y, Morimoto S, Kitano S, et al. Lysophosphatidylcholine causes Ca2+ influx, enhanced DNA synthesis and cytotoxicity in cultured vascular smooth muscle cells. Atherosclerosis 1995;112:69–76. [PubMed: 7772068]
20. Aiyar N, Disa J, Ao Z, et al. Lysophosphatidylcholine induces inflammatory activation of human coronary artery smooth muscle cells. Mol Cell Biochem 2007;295:113–120. [PubMed: 16896535]
21. Yamakawa T, Eguchi S, Yamakawa Y, et al. Lysophosphatidylcholine stimulates MAP kinase activity in rat vascular smooth muscle cells. Hypertension 1998;31:248–253. [PubMed: 9453311]
22. Yamakawa T, Tanaka S, Yamakawa Y, et al. Lysophosphatidylcholine activates extracellular signal-regulated kinases 1/2 through reactive oxygen species in rat vascular smooth muscle cells. Arterioscler Thromb Vasc Biol 2002;22:752–758. [PubMed: 12006386]

23. Hu Y, Chan E, Wang SX, Li B. Activation of p38 mitogen-activated protein kinase is required for osteoblast differentiation. Endocrinology 2003;144:2068–2074. [PubMed: 12697715]

24. Ducy P, Karsenty G. Two distinct osteoblast-specific cis-acting elements control expression of a mouse osteocalcin gene. Mol Cell Biol 1995;15:1858–1869. [PubMed: 7891679]

25. Shioi A, Nishizawa Y, Jono S, et al. Beta-glycerophosphate accelerates calcification in cultured bovine vascular smooth muscle cells. Arterioscler Thromb Vasc Biol 1995;15:2003–2009. [PubMed: 7583582]

26. Tanaka T, Sato H, Doi H, et al. Runx2 Represses Myocardin-mediated Differentiation and Facilitates Osteogenic Conversion of Vascular Smooth Muscle Cells. Mol Cell Biol 2008;28:1147–1160. [PubMed: 18039851]

27. Jones DC, Wein MN, Oukka M, et al. Regulation of adult bone mass by the zinc finger adapter protein Schnurri-3. Science 2006;312:1223–1227. [PubMed: 16728642]

28. Inoue T, Kawashima H. 1,25-Dihydroxyvitamin D3 stimulates 45Ca2+-uptake by cultured vascular smooth muscle cells derived from rat aorta. Biochem Biophys Res Commun 1988;152:1388–1394. [PubMed: 2837186]

29. Jono S, Nishizawa Y, Shioi A, Morii H. 1,25-Dihydroxyvitamin D3 increases in vitro vascular calcification by modulating secretion of endogenous parathyroid hormone-related peptide. Circulation 1998;98:1302–1306. [PubMed: 9751679]

30. Proudfoot D, Davies JD, Skepper JN, et al. Acetylated low-density lipoprotein stimulates human vascular smooth muscle cell calcification by promoting osteoblastic differentiation and inhibiting phagocytosis. Circulation 2002;106:3044–3050. [PubMed: 12473549]

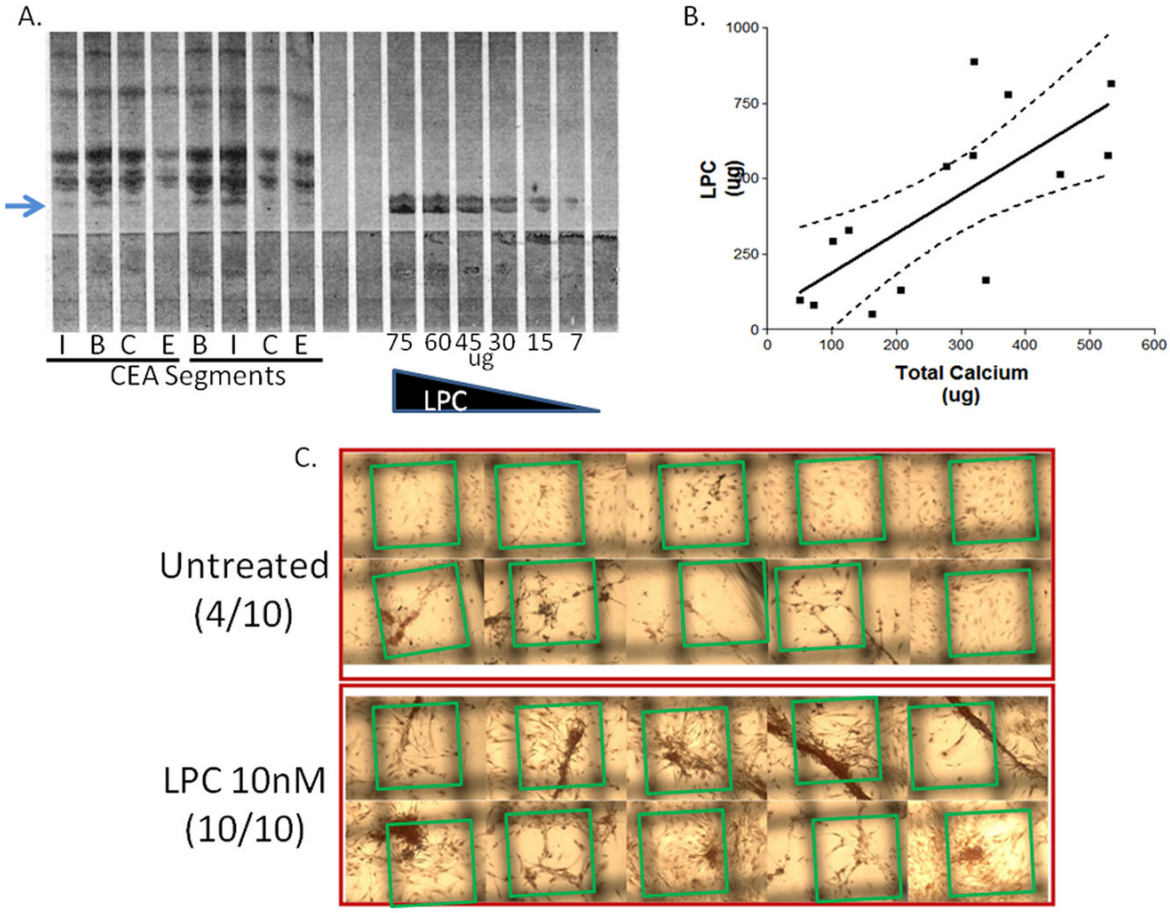

Figure 1. LPC correlates to CEA mineralization

(**A**) LPC abundance in human CEA segments; I, internal; B, bifurcation; C, common; E, external. LPC (μg) used as standard curve. Arrow = LPC (**B**) LPC (μg) correlates to CEA total calcium (soluble calcium + pelleted calcification) (μg). Linear regression with 95% confidence lines. n=14 (**C**) LPC induces VSMC mineralizations in culture. Morphometric analysis of calcific ridges, Alizarin Red S stain. Green boxes outline the edges of the uniform grid used to score positive mineralizations.

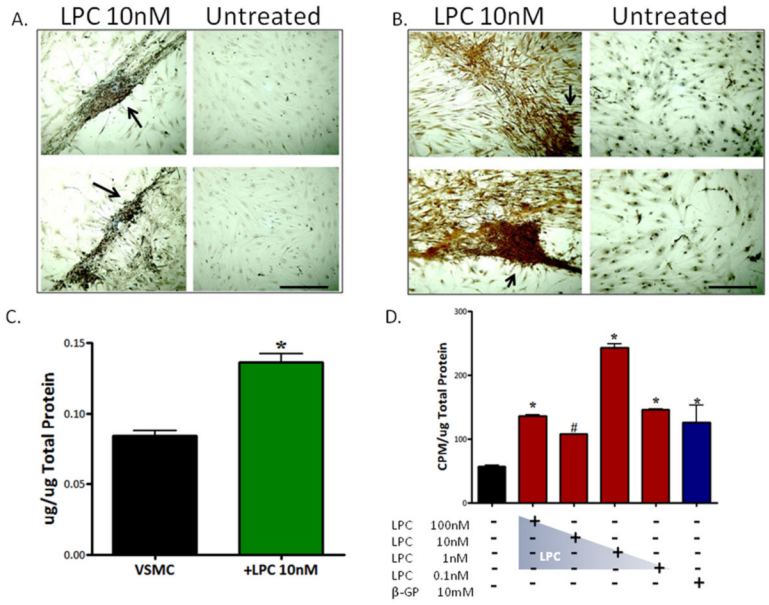

Figure 2. LPC-treated VSMCs produce calcium phosphate deposits in culture

(**A**) von Kossa stain, 14d, 4X. Arrows indicate calcium phosphate ridges. (**B**) Alizarin Red S calcium stain, 14d, 4X. Arrows indicate calcium structures. Scale bar = 200μm (**C**) Total phosphate levels; n=3, p<0.05, phosphate (μg) normalized to total protein (μg) (**D**) Calcium incorporation assay; $^{45}CaCl_2$, n=6,*p<0.01, #p<0.05. CPM was normalized to total protein (μg/μL) concentrations (CPM/μg total protein). Error bars represent ±SD.

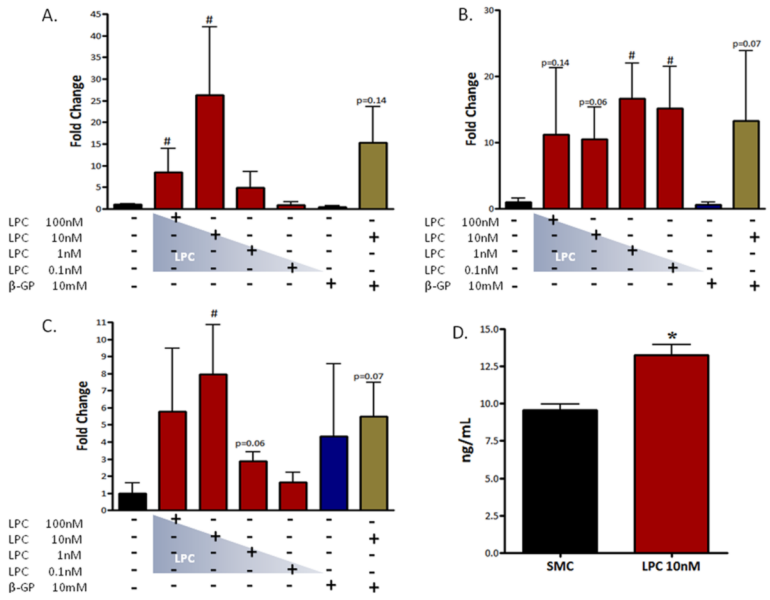

Figure 3. LPC induces osteogenic gene expression in VSMCs

A–C, Real-time PCR.14d, *n*=3-7. (**A**) Alkaline phosphatase. (**B**) Collagen 1α. (**C**) Osteopontin. (**D**) Osteopontin (protein) ELISA Assay, 14d, *n*=6. *$p<0.01$, # $p<0.05$. Error bars represent ±SD.

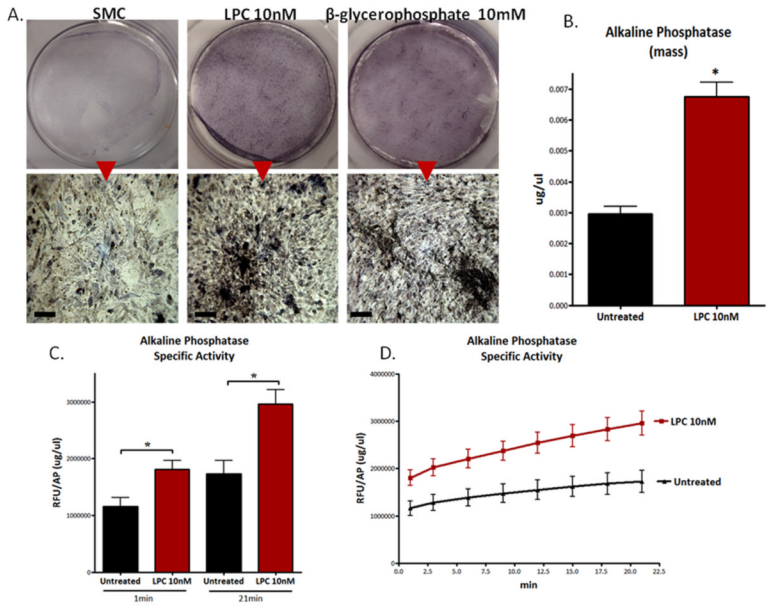

Figure 4. LPC induces alkaline phosphatase activity in VSMCs

(**A**) Alkaline phosphatase activity assay. 1X upper panels; 4X lower panels. Scale bar = 200μm. (**B**) Alkaline phosphatase mass. *p<0.01 (**C**) Alkaline phosphatase specific activity (RFU/AP mass (μg/μL)) at 1 and 21 min (**D**) Alkaline phosphatase specific activity over time.

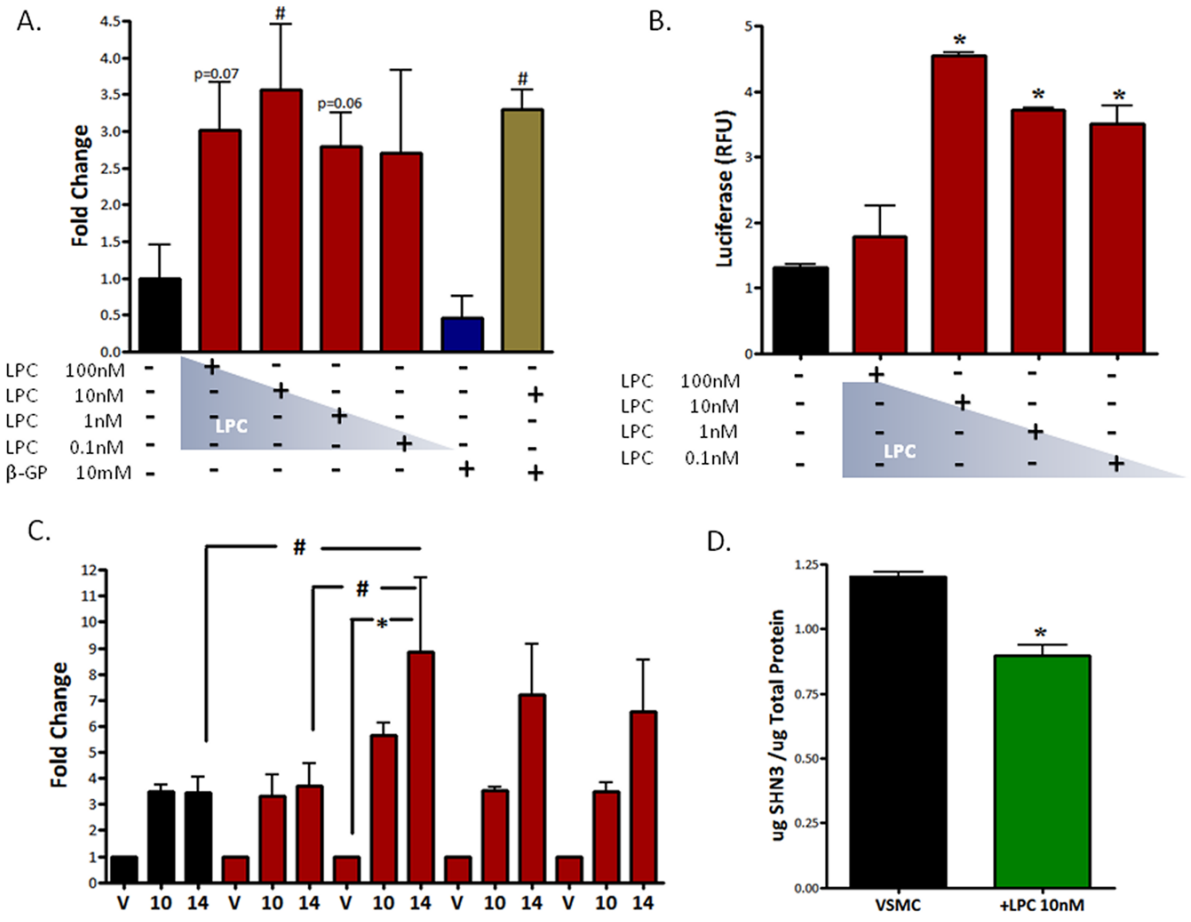

Figure 5. RUNX2 expression and transcriptional activity are increased in LPC-treated VSMCs

(**A)** Real-time PCR, RUNX2, 14d, *n*=3-7, # p<0.05. (**B**) RUNX2-Luciferase Reporter Assay; 14d, *n*=3, **p*<0.001. RLU, relative luciferase units. (**C)** Temporal Luciferase Assay, 10d-14d, *n*=3, **p*<0.01, # p<0.05. Error bars represent ±SD. (**D**) Schnurri 3 (protein) ELISA; n=3 *p<0.05. Schnurri 3 protein (μg) normalized to total protein (μg).